

AIP | Conference Proceedings

Atomic physics of shocked plasma in winds of massive stars

Maurice A. Leutenegger, David H. Cohen, and Stanley P. Owocki

Citation: *AIP Conf. Proc.* **1438**, 111 (2012); doi: 10.1063/1.4707864

View online: <http://dx.doi.org/10.1063/1.4707864>

View Table of Contents: <http://proceedings.aip.org/dbt/dbt.jsp?KEY=APCPCS&Volume=1438&Issue=1>

Published by the [American Institute of Physics](http://www.aip.org).

Additional information on AIP Conf. Proc.

Journal Homepage: <http://proceedings.aip.org/>

Journal Information: http://proceedings.aip.org/about/about_the_proceedings

Top downloads: http://proceedings.aip.org/dbt/most_downloaded.jsp?KEY=APCPCS

Information for Authors: http://proceedings.aip.org/authors/information_for_authors

ADVERTISEMENT


AIP Advances

Submit Now

**Explore AIP's new
open-access journal**

- **Article-level metrics
now available**
- **Join the conversation!
Rate & comment on articles**

Atomic Physics Of Shocked Plasma In Winds Of Massive Stars

Maurice A. Leutenegger^a, David H. Cohen^b and Stanley P. Owocki^c

^a*NASA/Goddard Space Flight Center, Greenbelt, MD 20771; CRESST/UMBC*

^b*Swarthmore College, Swarthmore, PA 19081*

^c*Bartol Research Institute, University of Delaware, Newark, DE 19716*

Abstract. High resolution diffraction grating spectra of X-ray emission from massive stars obtained with Chandra and XMM-Newton have revolutionized our understanding of their powerful, radiation-driven winds. Emission line shapes and line ratios provide diagnostics on a number of key wind parameters. Modeling of resolved emission line velocity profiles allows us to derive independent constraints on stellar mass-loss rates, leading to downward revisions of a factor of a few from previous measurements. Line ratios in He-like ions strongly constrain the spatial distribution of X-ray emitting plasma, confirming the expectations of radiation hydrodynamic simulations that X-ray emission begins moderately close to the stellar surface and extends throughout the wind. Some outstanding questions remain, including the possibility of large optical depths in resonance lines, which is hinted at by differences in line shapes of resonance and intercombination lines from the same ion. Resonance scattering leads to nontrivial radiative transfer effects, and modeling it allows us to place constraints on shock size, density, and velocity structure.

Keywords: stars: mass-loss; stars: early-type; stars: winds, outflows; X-rays: stars; radiative transfer

PACS: 32.30.Rj; 97.10.Ex; 97.10.Me; 97.20.Ec

INTRODUCTION

Massive stars are of great importance in the cosmic cycle of baryonic matter: ejecta from core collapse supernovae are one of the main sources of enrichment of heavy elements in the universe; radiation from massive stars, which are the first stars to appear in a star formation event, has a profound effect on the surrounding interstellar medium (ISM) and thus on the entire star formation process; and their powerful winds further influence the ISM through input of kinetic energy, and in later evolutionary stages, enriched material from the former core exposed by mass-loss in earlier stages. The winds of massive stars are also important for their effect on the evolution of the star itself. The fractional mass loss over the core hydrogen burning lifetime of the star can be significant, and in later evolutionary stages it is even greater.

The winds of massive stars are driven by radiation pressure in spectral lines, which is a result of their enormous luminosity ($10^5 - 10^6 L_{\odot}$). The effectiveness of line driving is multiplied in the highly supersonic flow as saturated absorption lines are Doppler shifted out of their own shadow in the acceleration zone of the wind, allowing for an increase in momentum transfer in optically thick lines by a factor of v_{∞}/v_{th} . The winds of massive stars are thus unique laboratories for studies of radiation hydrodynamics.

Radiative line driving is unstable to perturbations. Although the instability is damped

near the base of the wind by the scattered radiation field, hydrodynamic simulations show that the instability leads to extreme inhomogeneities in the wind (clumping), as well as energetic shocks. This results in significant X-ray emission, which has great diagnostic utility in studies of massive star winds.

The single most important measurable parameter of massive star winds is the mass-loss rate, since this sets the scale of evolutionary and ISM feedback effects. Although there are many observational diagnostics of mass loss (e.g. H α recombination lines, radio free-free emission, UV P Cygni absorption profiles [1, 2]), all of them are dependent on modeling assumptions, and thus potentially subject to systematic errors. X-ray emission line profiles observed using high-resolution diffraction grating spectrometers provide an alternative mass-loss rate diagnostic that does not share the same systematic errors as other techniques. X-ray line profiles are insensitive to density inhomogeneity, non-monotonic velocity fields, and the ionization of the bulk of the wind.

X-RAY LINE PROFILE MODELING

Owocki and Cohen [3] have described a formalism for calculating massive star X-ray emission line profiles. The wind is treated as a two-component fluid, with a small fraction of the wind heated to X-ray emitting temperatures and a dominant cool component which absorbs X-rays. X-rays emitted from the near hemisphere of the wind are blueshifted and suffer less absorption, while X-rays emitted from the back hemisphere are redshifted and more absorbed. The degree of absorption is characterized by the parameter $\tau_* \equiv \kappa \dot{M} / 4\pi R_* v_\infty$, where $\kappa(\lambda)$ is the microscopic opacity of the wind to X-rays, R_* is the stellar radius, v_∞ is the wind terminal velocity, and \dot{M} is the stellar mass-loss rate. This can also be written as $\tau_* = \kappa \Sigma_*$, with $\Sigma_* \equiv \dot{M} / 4\pi R_* v_\infty$ the characteristic wind mass column density. Example model profiles are shown in the left panel of Figure 1. τ_* is varied from 0 - 100, with increasing characteristic optical depth corresponding to more blueward skewed profiles. This variation in profile shape with wind optical depth is the basis for the use of X-ray line profiles as a mass-loss rate diagnostic. The right panels of Figure 1 show an example of a model fit to the Fe XVII 15.014 Å line of the prototypical O star ζ Pup. The statistical uncertainty on the derived value of τ_* for this line is of order 10%, showing that even data of moderate statistical quality can provide a powerful mass-loss rate diagnostic, provided that systematic effects are well understood.

HE-LIKE TRIPLET LINE RATIOS

Line ratios of He-like ions have been used extensively in laboratory and astrophysical plasmas as density and UV field diagnostics [4, 5]. The lowest lying excited state, $1s2s\ ^3S_1$, is metastable, so that collisional or photoexcitation to the $1s2p\ ^3P$ levels can compete with decay to ground. This alters the observed ratio of the intercombination ($1s^2\ ^1S_0 - 1s2p\ ^3P$; x, y , or alternately i) to forbidden ($1s^2\ ^1S_0 - 1s2s\ ^3S_1$; z , or alternately f) line strengths. Because the decay of the $1s2s\ ^3S_1$ state to ground is an M2 transition, the rate scales with Z^{10} , so that by observing He-like ions over a range of a factor of two in atomic number (nitrogen to silicon), we probe three orders of magnitude in decay

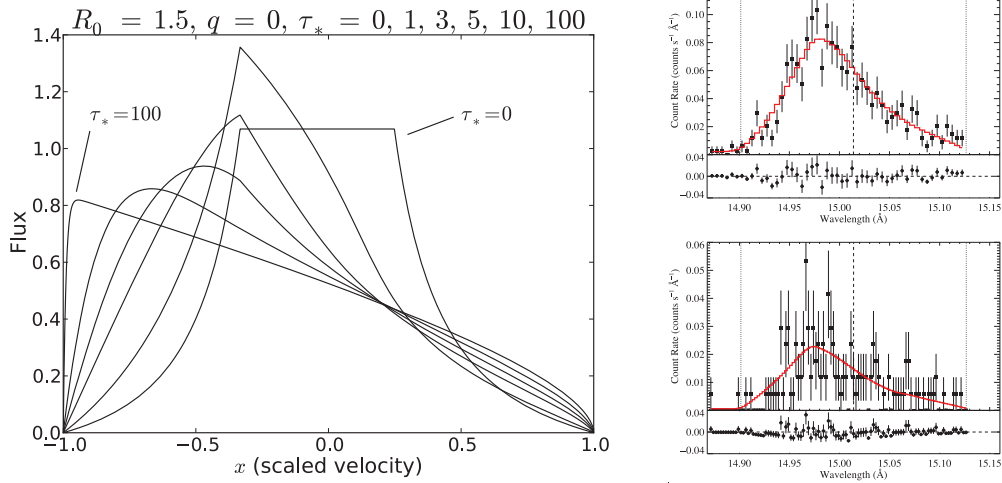


FIGURE 1. Left panel: comparison of line profiles with different characteristic optical depths τ_* . Right panel: *Chandra* MEG (top) and HEG (bottom) data for Fe XVII 15.014 Å fit with a line profile model (red curve) [7].

rate.

Plasma densities in O star winds are too low to affect f/i ratios, but the photospheric UV field has a strong effect. The UV field strength, and thus the f/i ratio depends on distance from the star. A calculation of this effect is shown for different He-like ions in the wind of the early O star ζ Pup in the left panel of Figure 2. It is not possible to invert the observed f/i ratio to obtain a localized radius of plasma formation, simply because the X-ray emitting plasma is spread out over a large range in radii. However, the correct radial dependence of the line ratio can easily be incorporated into a line profile model, yielding a model that predicts both line shape and line ratios with no additional free parameters [6]. An example of such a model fit is given in the right panel of Figure 2. Such models have been applied to X-ray spectra of O stars, resulting in good agreement.

MASS LOSS RATE DIAGNOSTICS

By measuring the characteristic optical depth τ_* for every reasonably strong emission line in the X-ray spectrum of an O star, it is possible to make a precise measurement of the mass-loss rate. We have performed such a measurement for ζ Pup, shown in Figure 3 [7]. We plot the measured values of τ_* as a function of wavelength, together with two model optical depths with different mass-loss rates. The model optical depths are calculated using the equation $\tau_* = \kappa(\lambda)\Sigma_*$, taking the mass-loss rate as the only changeable parameter. The dashed line shows the model corresponding to the upper-limit mass-loss rate inferred from radio free-free emission, while the solid line shows the model corresponding to the best fit to the X-ray data. The dominant uncertainty in our mass-loss rate determination is from uncertainty in the microscopic opacity model, which results from uncertainties in the elemental abundances and the ionization of helium.

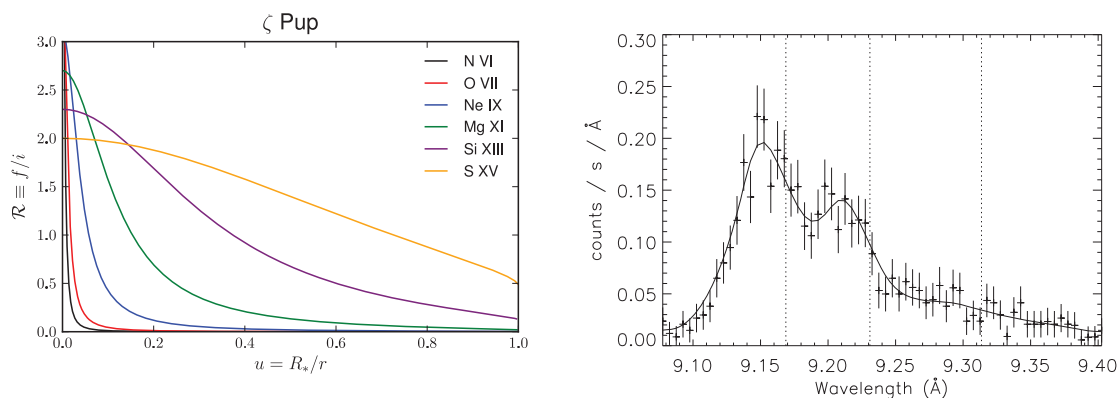


FIGURE 2. Left panel: dependence of f/i ratio in He-like triplets on distance from the photosphere of ζ Pup [6]. Right panel: Emission lines of Mg XI in the spectrum of ζ Pup, fit with a line profile model including the radial dependence of f/i ratio [6]. Rest wavelengths are indicated with vertical dashed lines. From left to right, the lines are resonance (w), intercombination (y), and forbidden (z).

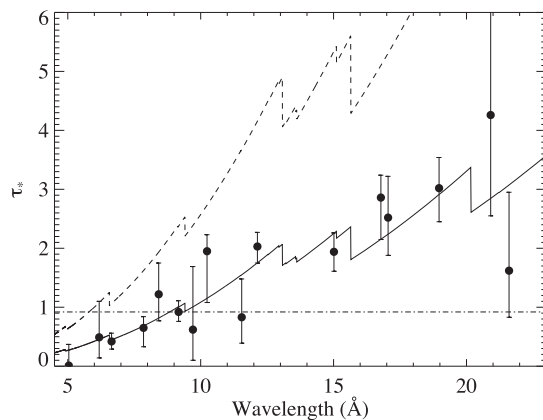


FIGURE 3. Measured characteristic optical depth τ_* for strong emission lines in the spectrum of ζ Pup plotted as a function of wavelength [7]. The shape of the model curves reflects the microscopic opacity of the wind. The dashed and solid lines correspond to mass-loss rates of $8.3 \times 10^{-6} M_{\odot} \text{ yr}^{-1}$ and $3.5 \times 10^{-6} M_{\odot} \text{ yr}^{-1}$, respectively.

RESONANCE SCATTERING

The resonance and intercombination lines from a He-like triplet are expected to have the same profile shape, since they both come from the same ion. Surprisingly, these two lines have been found to have different profile shapes for He-like triplets in some O star X-ray spectra. In the left panel of Figure 4, we show a model fit to the N VI triplet of ζ Pup [8]. The resonance line is more symmetric than the model, while the intercombination line is more asymmetric. This cannot be explained by the radial dependence of the f/i ratio, which is included in the model.

If strong resonance lines are optically thick, the radiative transfer depends on the velocity structure along the line of sight. This problem has been well studied in the

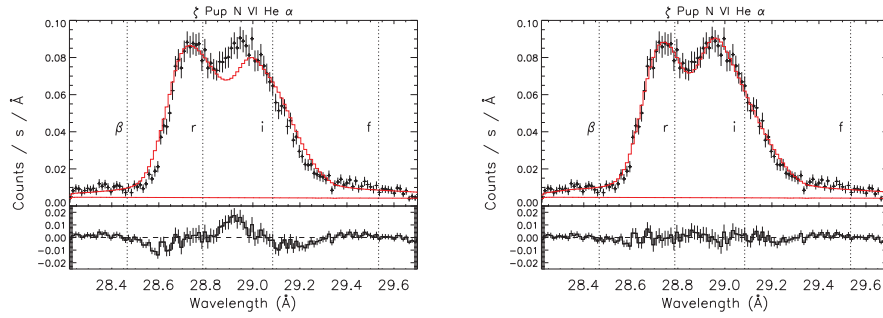


FIGURE 4. Fits to N VI He-like triplet of ζ Pup. A model with no resonance scattering (left panel) cannot fit the resonance and intercombination lines simultaneously, while a model including the effects of resonance scattering (right panel) fits well.

context of UV line profile modeling in O star winds. Radial photon escape is due to radial velocity gradients (dv/dr), while lateral photon escape is due to the spherical divergence of the wind (v/r), which results in lateral line-of-sight velocity gradients. In typical O star winds, lateral photon escape is favored for $r \gtrsim 2R_*$. Since lateral photon escape results in low observed Doppler shifts, strong resonance scattering in X-ray line formation results in more symmetric lines. This symmetrization effect only applies to resonance lines, which have large oscillator strengths, and not to intercombination or forbidden lines.

This effect can be seen in the models shown in Figure 5. The strength of resonance scattering is described by the characteristic Sobolev optical depth, $\tau_{0,*}$. Larger values of $\tau_{0,*}$ result in more symmetric profiles. This model has been fit to the N VI triplet of ζ Pup with $\tau_{0,*}$ as a free parameter, as shown in the right panel of Figure 4. The fit is greatly improved, indicating that resonance scattering is important in the formation of this profile. Evidence for this effect has been found in X-ray spectra of other O stars as well. However, detailed interpretation of resonance scattering effects are handicapped by the fact that we can only guess at the velocity structure in the X-ray emitting regions.

FE XVII LINE RATIOS

The X-ray spectrum of ζ Pup shows an anomaly which has not been observed in any other astrophysical X-ray spectrum to date. The ratio of $3s - 2p$ lines ($17.051 \text{ \AA} + 17.096 \text{ \AA}$) / (16.780 \AA) is typically found to be ~ 2.4 for a wide range of astrophysical sources, including coronal stars with a wide range of temperatures, and including all other O stars. However, in ζ Pup, this line ratio is ~ 1.4 . There is no obvious mechanism that would produce this effect. Photoexcitation of the metastable lowest lying excited state ($J = 2$) has been considered in a study of Fe XVII line ratios in the magnetic cataclysmic variable system EX Hya [9]; this cannot be effective in this case, because photoexcitation is most effective at connecting the upper levels of the 17.051 \AA and 17.096 \AA lines, respectively (via a manifold of $3p$ states). Resonance scattering is also probably not important for any of these lines, since none of them has a large oscillator strength.

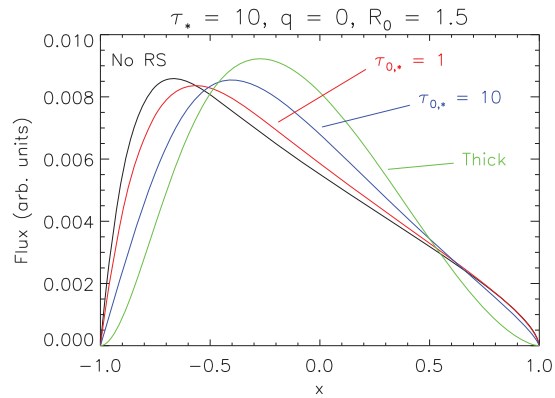


FIGURE 5. Model line profiles (flux as a function of scaled velocity x) showing the effect of resonance scattering. Larger values of the characteristic Sobolev optical depth ($\tau_{0,*}$) produce more symmetric profiles.

Resonance scattering also has little or no effect on line ratios.

One possible explanation for the observed line ratio is a near coincidence between either the 17.051 Å or 17.096 Å line and an inner-shell 2p-3d absorption line of a low charge state of iron with a large ion fraction in the bulk of the wind, such as Fe VI. Such inner-shell absorption lines have been observed in AGN warm absorber absorption spectra [10], and have been the subject of extensive theoretical and laboratory investigation [11, 12]; however, lower charge states have received less experimental attention and pose greater theoretical difficulties due to the larger number of electrons. If such a coincidence exists, then line emission from the X-ray emitting part of the wind may be efficiently destroyed in the cool bulk of the wind. This hypothesis may also explain why this effect is only observed in ζ Pup: if the charge balance of iron is significantly different for ζ Pup than for the other O stars that have been observed by XMM and *Chandra*, as might be expected from its higher effective temperature, then this absorption may only be important in ζ Pup.

ACKNOWLEDGMENTS

This work includes previously published results supported by NASA grants NNG04-GL76G, AR5-6003X, AR7-8002X, TM6-7003X, and NNG05GC36G.

REFERENCES

1. J. Puls, N. Markova, S. Scuderi, C. Stanghellini, O. G. Taranova, A. W. Burnley, and I. D. Howarth, *Astron. Astrophys.* **454**, 625 (2006).
2. A. W. Fullerton, D. L. Massa, and R. K. Prinja, *Astrophys. J.* **637**, 1025 (2006).
3. S. P. Owocki, and D. H. Cohen, *Astrophys. J.* **559**, 1108 (2001).
4. A. H. Gabriel, and C. Jordan, *MNRAS* **145**, 241 (1969).
5. G. R. Blumenthal, G. W. F. Drake, and W. H. Tucker, *Astrophys. J.* **172**, 205 (1972).
6. M. A. Leutenegger, F. B. S. Paerels, S. M. Kahn, and D. H. Cohen, *Astrophys. J.* **650**, 1096 (2006).

7. D. H. Cohen, M. A. Leutenegger, E. E. Wollman, J. Zsargó, D. J. Hillier, R. H. D. Townsend, and S. P. Owocki, *MNRAS* **405**, 2391 (2010).
8. M. A. Leutenegger, S. P. Owocki, S. M. Kahn, and F. B. S. Paerels, *Astrophys. J.* **659**, 642 (2007).
9. C. W. Mauche, D. A. Liedahl, and K. B. Fournier, *Astrophys. J.* **560**, 992 (2001).
10. M. Sako, S. M. Kahn, E. Behar, J. S. Kaastra, A. C. Brinkman, T. Boller, E. M. Puchnarewicz, R. Starling, D. A. Liedahl, J. Clavel, and M. Santos-Lleo, *Astron. Astrophys.* **365**, L168 (2001).
11. M. F. Gu, T. Holczer, E. Behar, and S. M. Kahn, *Astrophys. J.* **641**, 1227 (2006).
12. M. C. Simon, J. R. Crespo López-Urrutia, C. Beilmann, M. Schwarz, Z. Harman, S. W. Epp, B. L. Schmitt, T. M. Baumann, E. Behar, S. Bernitt, R. Follath, R. Ginzel, C. H. Keitel, R. Klawitter, K. Kubiček, V. Mäckel, P. H. Mokler, G. Reichardt, O. Schwarzkopf, and J. Ullrich, *Physical Review Letters* **105**, 183001 (2010).